Carbon 101 (2016) 281–289

Contents lists available at ScienceDirect

Carbon

journal homepage: www.elsevier.com/locate/carbon

First report of fumed alumina incorporation in carbon–carbon composite and the consequent improvement of the oxidation resistance and mechanical properties

Andi Wang, D.D.L. Chung*

Composite Materials Research Laboratory, University at Buffalo, State University of New York, Buffalo, NY, 14260-4400, USA

ARTICLE INFO

Article history:
Received 12 October 2015
Received in revised form
1 February 2016
Accepted 2 February 2016
Available online xxx

ABSTRACT

The first report of fumed alumina incorporation in carbon–carbon (C/C) composite is provided. Fumed alumina (0.5 vol.% solid alumina in the C/C, 15-nm average pore size, 100–200-nm squishable/conformable aggregates of nanoparticles) as a filler in unidirectional C/C (44 vol.% fibers, fabricated by 1000 °C 21-MPa hot-press mesophase-pitch carbonization) is as effective as one-cycle densification for decreasing the porosity (from 16% to 14%) and increasing the flexural modulus (from 52 to 68 GPa) and longitudinal hardness (from 2.7 to 5.5 GPa), and more effective than one-cycle densification for improving the flexural strength (to 330 vs. 280 MPa), longitudinal compressive modulus (to 38 vs. 30 GPa) and oxidation resistance. The positive mechanical/thermal effects of fumed alumina incorporation suggest pore structure refinement, due to the nanostructure and conformability of fumed alumina. Thus, a quality C/C is obtained at a low density (1.54 g/cm^3). Fumed alumina is more effective than organobentonite (3.3. vol.%, previously shown to serve unusually as both filler and binder) for improving the oxidation resistance and as effective as organobentonite for increasing the flexural strength/modulus, in spite of the higher porosity of its C/C (14% versus 12%). However, fumed alumina is inferior to organobentonite for increasing the toughness or longitudinal compressive modulus.

1. Introduction

Carbon–carbon (C/C) composites refer to continuous carbon fiber carbon-matrix composites. They are the dominant high-temperature lightweight structural materials, as used for reentry vehicles, missiles and aircraft brakes. In addition, they are used in biomedical and corrosion-resistant applications, due to the biocompatibility and chemical resistance of carbon. However, C/C suffers from high processing cost, which is due to the need to use multiple impregnation–carbonization cycles and methods such as chemical vapor infiltration (CVI) in order to achieve sufficient densification and hence adequate mechanical properties and oxidation resistance. In addition, they suffer from low ductility, due to the brittleness of the carbon matrix.

The incorporation of organobentonite particles in C/C increases the flexural strength, flexural modulus and oxidation resistance, such that the need for densification is reduced [1,2]. The effectiveness of the organobentonite incorporation is because the organobentonite serves as both reinforcement and binder, such that the organobentonite is converted to a ceramic-carbon nanostructured hybrid (86 vol.% ceramics, 14 vol.% carbon) during the concurrent pyrolysis of the organic component of the organobentonite and the carbon matrix precursor used in making the C/C [1].

The incorporation of SiC in C/C by liquid silicon infiltration increases the flexural strength from 82 to 120 MPa [3]. The incorporation of carbon black in C/C increases the flexural strength from 15 to 42 MPa, in addition to increasing the true density from 1.52 to 1.67 g/cm^3 and decreasing the open porosity from 9% to 8% [4]. On the other hand, the incorporation of SiC in C/C by carbothermal reduction of SiO_2 to SiC (mainly SiC whiskers) decreases the flexural strength [5] and the incorporation of SiC whiskers in C/C by the growth of the whiskers on a carbon fabric also decreases the flexural strength [6]. The incorporation of carbon nanofibers in C/C by mixing the nanofibers with the precursor resin has negligible effect on the interlaminar shear strength [7].

Filler incorporation is much less expensive than in-situ filler

* Corresponding author.
E-mail address: ddlchung@buffalo.edu (D.D.L. Chung).
URL: http://alum.mit.edu/www/ddlchung

http://dx.doi.org/10.1016/j.carbon.2016.02.008
0008-6223/

growth. The incorporation of carbon nanotubes (CNT) in C/C by in-situ growth of CNT on the carbon fibers increases the flexural strength from 179 to 233 MPa and increases the flexural modulus from 33 to 58 GPa, in addition to increasing the true density [8].

Alumina is attractive for its high melting temperature, high modulus and stability even in the presence of oxygen and heat. In contrast, carbon becomes oxidized in the presence of oxygen and heat.

Fumed alumina is produced in a flame, commonly involving the reaction [9].

$$2AlCl_3 + 3H_2 + 1.5\ O_2 \rightarrow Al_2O_3 + 6\ HCl,$$

where aluminum chloride, hydrogen and oxygen are the reagents. Fumed alumina is in the form of aggregated nanoparticles. Upon compaction, the aggregates are squished (compressed), resulting in mechanical interlocking among the particles and the formation of a sheet that follows the topography of the surface on which the compaction is conducted. This squishability enables conformability and spreadability, which are valuable for tightening interfaces, thereby reducing the porosity in the resulting composite. Fumed metal oxides are superior to carbon black in the ability to withstand high temperatures in the presence of oxygen. Carbon black has been incorporated in C/C for enhancing the mechanical properties [4]. However, fumed metal oxides have not. On the other hand, fumed alumina has been previously incorporated in organic materials [10–12]. In particular, due to its conformability, a thermal paste containing fumed alumina excels as a thermal interface material for improving the thermal contact between two surfaces [11,12].

The primary objective of this work is to investigate the effects of fumed alumina incorporation on the oxidation resistance and mechanical properties of C/C. The secondary objective is to compare the effect of fumed alumina incorporation and that of organobentonite incorporation.

2. Experimental methods

2.1. Materials

The continuous carbon fibers are Thornel P-25X mesophase-pitch-based fibers (without sizing and without twist) from Cytec Industries Inc, Woodland Park, NJ. It is in the form of 2000-filament tows, with tensile strength 1.56 GPa, tensile modulus 159 GPa, and density 1.92 g/cm^3.

The pitch used as the carbon matrix precursor for both the composite fabrication and the subsequent optional densification process is mesophase pitch powder, which is a type which has been solvated, i.e., plasticized with a proprietary solvent (15.5%) that contains polynuclear aromatic compounds and allows the mesophase to be easily melted and pumped and be readily dried. The dry melting point (solvent free) of the pitch is about 395 °C. In a closed environment, the pitch starts to soften at around 220 °C. (If the pitch is heated in the open, the solvent will begin to leave well before the mesophase melts, leaving a high-melting material that is hard to handle.) The coking value is 0.80. The pitch is from Conoco Corporation. It is different from the pitch used in prior work [1].

Two types of filler are used in this work, namely fumed alumina and organobentonite. The organobentonite case has been previously reported [1], but this paper provides more in-depth analysis and uses this case for the sake of comparison. The mass proportions of the constituents in each type of composite studied are shown in Table 1.

The fumed alumina is in its untreated state, as provided by Cabot Corp. (Billerica, MA) under the designation SpectrAl 51. It is a white fluffy powder with specific gravity 3.6 at 20 °C and melting point about 2000 °C. It has specific surface area 55 m^2/g, aggregate size 100–200 nm, Al_2O_3 content exceeding 99.8 wt.% and a positive surface charge. The positive charge is probably due to the dissociation of ionogenic groups on the particle surface and/or the differential adsorption from solution of ions of different charges into the surface region during the fumed alumina fabrication. The aggregates form loose, micrometer-sized agglomerates. The mass loss on heating is less than 1.5 wt.% at 105 °C. The fumed alumina is a mixture of theta, delta, gamma and amorphous forms of alumina. Its morphology is shown by the scanning electron microscope (SEM) photograph in Fig. 1(a).

Table 1
C/C composite constituent mass proportions.

Filler	Densification	Mass fraction (%)		
		Fiber	Matrix[a]	Filler
None	No	55.56 ± 0.70	44.44 ± 0.56	0
None	Yes	55.56 ± 0.70	44.44 ± 0.56	0
Fumed alumina	No	54.95 ± 0.97	43.95 ± 0.77	1.10 ± 0.01[b]
Organobentonite	No	51.98 ± 0.68	41.58 ± 0.54	6.44 ± 0.08

[a] Based on the mass of the pitch and the carbon yield of 0.80 ± 0.01 for the pitch.
[b] The fumed alumina and pitch powder are in the mass ratio of 1:50.

Fig. 1(b) shows that the pores in a fumed alumina compact (compacted at 200 kPa) are mainly <50 nm in size. However, there are pores that exceed 100 nm in size, probably due to the interface between the fumed alumina aggregates. Nitrogen adsorption (Fig. 1(c) and (d)) shows that the specific surface area is 60.4 ± 0.1 and 54.8 ± 0.1 m^2/g before and after compaction, respectively; the average pore size (by the BJH Method, over the pore size range from 1 to 200 nm) is 14.8 and 14.5 nm before and after compaction, respectively; the cumulative pore volume (by the BJH Method, over the pore size range from 1 to 200 nm) is 0.213 and 0.166 cm^3/g before and after compaction, respectively. These observations mean that the compaction only slightly decreases the specific surface area and the pore size. The hysteresis in the adsorption-desorption isotherms shows that the fumed alumina is mesoporous, with the occurrence of capillary condensation, both before and after compaction. The slightly larger adsorption-desorption hysteresis area after compaction than before compaction is attributed to the consolidated structure after compaction hindering the out-diffusion of the desorbed gas.

The organobentonite (organobentonite, called known as organoclay or nanoclay) used is the same as that in prior work [1,13]. It is montmorillonite that has been intercalated with a dimethyl hydrogenated-tallow ammonium salt (dimethyl, dihydrogenated tallow) with chloride anions (Fig. 2) via a cation exchange process. The hydrogenated tallow involves ~65% fatty acids with 18 carbon atoms in the alkyl carbon chain, ~30% fatty acids with 16 carbon atoms in the chain, and ~5% fatty acids with 14 carbon atoms in the chain. The cation exchange capacity is 125 cmol/kg. The density is 1.66 g/cm^3. The loss on ignition is 43 wt%. The particles are white, with size such that 10% is less than 2 μm, 50% is less than 6 μm and 90% is less than 13 μm. Each layer is 1 nm thick and 70–150 nm across, with an aspect ratio 70–150. If it were exfoliated, the specific surface area would exceed 750 m^2/g. The basal spacing d_{001} = 31.5 Å [1]. This organobentonite is the product designated Cloisite 15A, as provided by Southern Clay Products, Inc., Gonzales, TX.

The hot-pressing of organobentonite particles in the absence of a binder or fiber has been previously shown to provide a monolithic ceramic-carbon hybrid solid that exhibits high flexural modulus and strength, low porosity and high oxidation resistance [1]. This behavior is a consequence of the organobentonite being able to

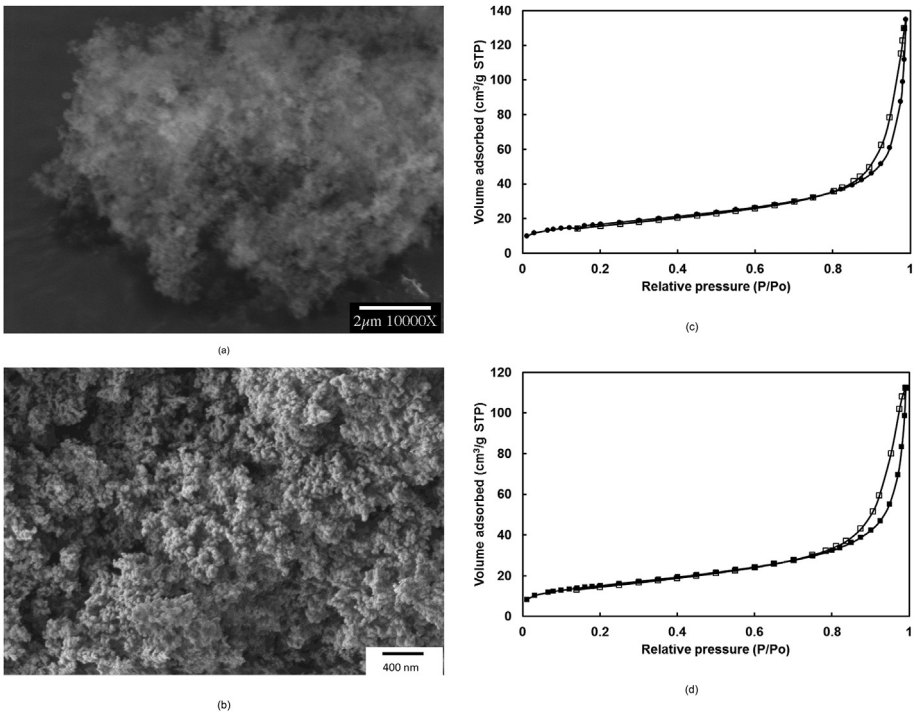

Fig. 1. Structure of fumed alumina before and after compaction. (a) SEM photograph of the fumed alumina prior to compaction. (b) SEM photograph of fumed alumina after compaction, with the view being the plane perpendicular to the direction of compaction. The microstructure is the same for the view of the side plane that contains the direction of compaction. (c) Adsorption-desorption isotherms of fumed alumina before compaction, with the lower curve being the adsorption curve and the upper curve being the desorption curve. (d) Adsorption-desorption isotherms of fumed alumina after compaction at 200 kPa, with the solid symbols for the adsorption curve and the open symbols for the desorption curve.

serve as a binder. Therefore, the incorporation of organobentonite particles in a C/C composite provides strengthening, due to the organobentonite serving as both a binder and a reinforcing filler [1].

2.2. Composite fabrication

The fumed alumina and pitch powder in the mass ratio of 1:50 are dry mixed in a ball mill (without grinding balls in order to avoid squishing or compacting the fumed alumina) for 24 h for the purpose of initial mixing. Then the mixture is dispersed in water that contains 0.1 wt.% dissolved poly(ethylene oxide) (PEO, a surfactant), such that the dispersion contains 10 wt.% alumina-pitch mixture. The dispersion is stirred manually for 10–20 min, followed by 2.0 h of magnetic stirring, in order to achieve an adequate degree of dispersion. The carbon fiber tow is immersed in the dispersion for 3.0 h in order for the tow to be coated with the alumina-pitch mixture.

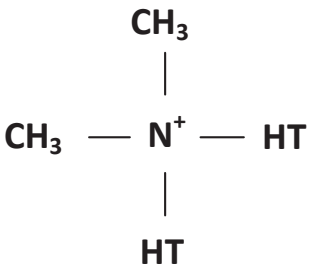

Fig. 2. An organocation in the form of a dimethyl hydrogenated-tallow ammonium. The abbreviation HT means hydrogenated tallow.

The mass ratio of the immersed fibers to pitch (in the dispersion) to fumed alumina (also in the dispersion) is 50:50:1. This proportion is such that the entirety of the liquid-based dispersion is consumed in coating the immersed fibers. Thus, the mass ratio of the fibers to pitch to fumed alumina in the prepreg is also 50:50:1.

After removal of the tow from the dispersion, the tow is placed on a Teflon (polytetrafluoroethylene) sheet, such that 17 tows are manually aligned to form a prepreg sheet of size 290 × 38 mm. Multiple sheets are made.

After this, the prepreg sheets are cut into discs of diameter 31.8 mm. A total of 8 discs are unidirectionally stacked to form a cylinder, which is allowed to dry in air at room temperature for 24 h, followed by hot pressing in a graphite mold under a nitrogen purge at a flow of 70 ml/min for the purpose of pyrolysis (carbonization). The temperature is first raised from room temperature (20 °C) to 220 °C at a heating rate of 5 °C/min without pressure application. After this, the temperature is maintained at 220 °C for 30 min without pressure application to allow solvent evaporation and oxygen in-diffusion. Then the temperature is increased from 220 to 370 °C at a heating rate of 5 °C/min without uniaxial pressure application. After this, the uniaxial pressure is increased to 5 MPa and the temperature is maintained at 370 °C for 4 h for the purpose of pitch stabilization. Then, under a nitrogen flow of 80 ml/min, the temperature is raised to 1000 °C at a heating rate of 5 °C/min with the uniaxial pressure maintained at 21 MPa. Subsequently, under nitrogen flow, the temperature is maintained at 1000 °C and the pressure maintained at 21 MPa for 30 min for the purpose of carbonization. After this, cooling is conducted naturally in the furnace under nitrogen in the absence of applied pressure until the temperature has reached room temperature. Imperfect alignment of the fibers necessarily occurs to a degree.

2.3. Testing

2.3.1. Thermal stability evaluation

The thermal stability is evaluated under purging nitrogen by thermogravimetric analysis (TGA) using a thermogravimetric analyzer (TGA 7, Perkin–Elmer Corp.). The TGA testing is conducted after removal of the moisture by heating at 110 °C for 2 h (This moisture removal step was not conducted in prior work [1], thus causing differences in the data between this work and the prior work.) In spite of the controlled nitrogen purge, air is present to a degree. The weight is measured at a heating rate of 5 °C/min from room temperature to 1000 °C.

2.3.2. Microstructural analysis

The microstructure of the fumed alumina and the C/C containing fumed alumina (without densification) was examined by microscopy, including SEM and optical microscopy. For the C/C, examination was directed at the cross-section of the composite after mechanical polishing. Please refer to the prior work [1] for the microstructure of the C/C without filler and without densification, C/C without filler but with densification, and C/C with organobentonite incorporation (without densification),

Measurement of the specific surface area and pore size distribution is conducted by isothermal gas adsorption, using nitrogen and the Micromeritics ASAP 2010 physisorption analyzer. By measuring the volume of nitrogen adsorbed onto a specimen at different pressures, the total pore volume and surface area in the specimen are determined. The pore size distribution is inferred from the adsorption isotherm using the well-known BJH (Barrett–Joyner–Halenda) Method. In addition, SEM is conducted to observe the pore morphology.

2.3.3. Mechanical testing under flexure

Static flexural testing up to failure is conducted under three-point bending with the fibers along the longitudinal direction of the unidirectional composite beam. The span is 20 mm. A hydraulic mechanical testing system (MTS Systems Corp., Eden Prairie, MN) is used. Two beam-shaped specimens are obtained from each 8-lamina composite disc by cutting along the diameter and along two parallel lines, so that each specimen has a width ranging from 9.1 to 10.3 mm, as separately measured for each specimen. Two discs were separately fabricated, with two specimens tested for each disc. The flexural ductility is taken as the flexural strain at the maximum stress in the stress–strain curve up to failure. The flexural toughness is the area under the stress–strain curve, with the area including the tail up to zero stress.

2.3.4. Instrumented indentation testing

Instrumented indentation testing (nanoindentation) is performed in accordance with the ASTM E2546 standard method. The equipment is a nanoindenter system (MTS Systems Corporation, Model XP) equipped with a diamond Berkovich indenter tip, which has a triangle-pyramidal shape and an angle of 77°. The tip radius is of the order of 50–150 nm. Testing is conducted during loading and subsequent unloading up to various maximum loads, under load control, with the force and displacement continuously measured in real time. Force and displacement are continuously measured in real time during loading and unloading by using two separate high-resolution devices (actuators/sensors). Indentation testing is conducted in the longitudinal direction, i.e., the fiber direction. The maximum load during indentation is fixed at values ranging from 10 to 40 mN. The loading rate is 1.00 μN/s. In each loading cycle, the maximum load is held for 3.0 s before unloading.

The reduced modulus E_r is needed to calculate the elastic modulus E of the specimen. The equation to calculate the reduced modulus E_r is [14].

$$E_r = \frac{S\sqrt{\pi}}{2\beta\sqrt{A}} \tag{1}$$

where S is the slope of the initial portion of the load–displacement curve during unloading and is known as the contact stiffness, which includes contributions from both the material being tested and the response of the test device. The dimensionless geometric parameter β in Eq. (1) is typically around 1; it is equal to 1.034 for the Berkovich tip. The quantity A in Eq. (1) is the projected area of the indentation at the contact depth. After obtaining the E_r using Eq. (1), the specimen modulus E can be calculated by using the equation below [14], which is based on contact mechanics [15]:

$$\frac{1}{E_r} = \frac{(1-\nu^2)}{E} + \frac{(1-\nu_i^2)}{E_i}, \tag{2}$$

where E_i and ν_i are the elastic modulus and the Poisson's ratio of the indenter tip respectively and ν is the Poisson's ratio of the specimen. For a diamond indenter tip, E_i is 1140 GPa and ν_i is 0.07. For most materials, ν is typically around 0.3. For clay, the value is 0.42 [16]. For graphite, the value is 0.18 [17].

The hardness of the test surface (H) is determined using the equation [14]

$$H = P/A, \tag{3}$$

where P is the maximum load applied to the test surface and A is the projected area at the maximum load. This hardness is usually higher than the microhardness based on the dimensions of the permanent indent after unloading [18], because it is based on the area at the maximum load.

For each specimen and each value of the selected maximum load, testing is conducted at ten different points, and the data scatter (±range) is thus determined for each of the reported quantities, which include the modulus, the hardness, the maximum displacement and the displacement per unit load (i.e., the maximum displacement divided by the maximum load).

3. Results and discussion

3.1. Oxidation resistance

Table 2 and Fig. 3 show that the composite with fumed alumina incorporation is superior to that with organobentonite incorporation in the oxidation resistance. It is also superior to the composite without filler but with densification. The superior oxidation resistance of the composite with fumed alumina occurs in spite of the relatively high porosity (14% for the composite with fumed alumina, compared to 12% for the composite with organobentonite, Table 2). This is probably because the porosity in the composite with fumed alumina is dominated by closed porosity that is associated with the nanopores in the squished fumed alumina aggregates (Fig. 1(b)). The squishability has been previously shown to cause the fumed alumina to be highly compactable

Table 2
Fractional weight loss of C/C composites upon heating at various temperatures.

Filler	Densification	400 °C	600 °C	800 °C	900 °C
None	No	0.256%	0.440%	0.785%	1.024%
None	Yes	0.136%	0.223%	0.469%	0.659%
Fumed alumina	No	0.118%	0.206%	0.441%	0.623%
Organobentonite	No	0.256%	0.341%	0.562%	0.760%

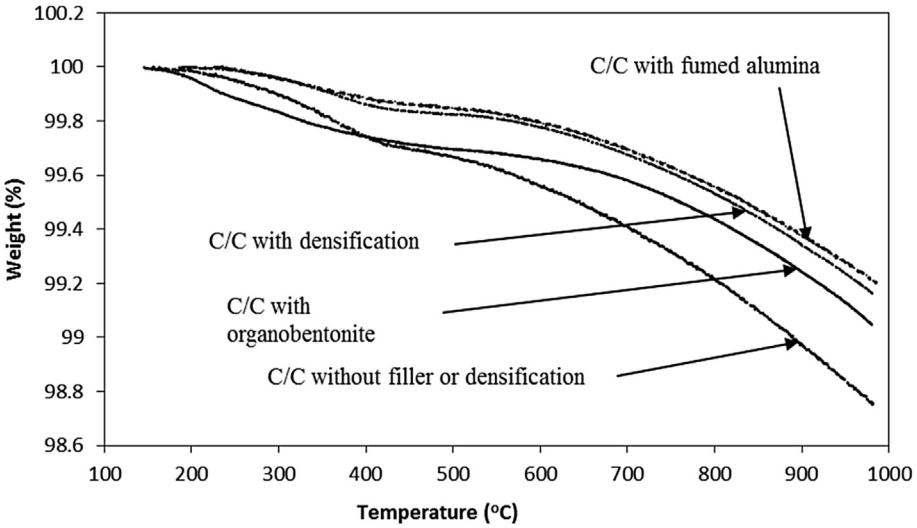

Fig. 3. Fractional weight of C/C composites during heating.

upon uniaxial compression, with the solid volume fraction of the compact increasing with increasing compaction pressure. For example, the solid volume fractions are 6.6%, 7.1%, 8.2% and 12.2% for compaction pressures of 50, 75, 100 and 200 kPa respectively [19]. For the pressure of 21 MPa used in the hot pressing of this work, the solid volume fraction in the fumed alumina compact is greater than 12.2%, i.e., the air volume fraction is less than 87.8%, or ratio of the air volume to solid alumina volume is less than 7. Even for the maximum ratio of 7, the volume fraction of 0.5% for the solid alumina in the C/C corresponds to a volume fraction of 3.5% for the air in the fumed alumina in the C/C. The value of 3.5% is much below the total porosity of 14% for the C/C with fumed alumina. Hence, the porosity in this C/C is dominated by that of the matrix (including the fiber-matrix interface), with the porosity inside the fumed alumina contributing to a minor degree. In other words, the fumed alumina mainly reduces the porosity of the matrix in terms of both the total pore volume and the mean pore size, with the introduction of nanoscale porosity by its presence making a minor contribution to the overall porosity of the C/C. Furthermore, the squishability enhances the conformability of the fumed alumina to the surface of the carbon fiber, thereby probably reducing the open porosity. In contrast, organobentonite is not squishable and, after hot pressing, is not porous [1], and the composite with organobentonite incorporation is inferior to the composite without filler but with densification. Densification improves the oxidation resistance, as expected and as shown by the composite without filler.

3.2. Composite structure and mechanical properties

Table 1 shows the mass proportions of the constituents in each of the four types of C/C. The mass proportion of the carbon matrix is based on the mass of the pitch and the carbon yield of 0.80 ± 0.01 for the pitch. The fiber mass fraction is higher than the matrix mass fraction. The filler mass fraction is much lower than the fiber or matrix mass fraction. The composites with filler have lower values of the matrix mass fraction than those without filler. The filler mass fraction is much higher for organobentonite than fumed alumina.

A composite consists of carbon fibers, carbon matrix, the solid part of the filler (if any) and the porosity, with the porosity including pores of all sizes, whether the pores are open or closed. Hence,

$$1 = V_f + V_m + V_h + \text{porosity}, \quad (4)$$

where V_f, V_m and V_h are the volume fractions of the fibers, matrix and filler respectively. The volume fractions of the constituents and the porosity can be obtained by calculation [1] based on the Rule of Mixtures for the density, the constituent mass proportions (Table 1) and the known densities of the constituents. In particular, the density of the carbon fibers is 1.920 ± 0.005 g/cm^3; the density of the alumina in the fumed alumina is 3.6 g/cm^3. Eq. (1) gives the values of the fiber volume fraction shown in Table 3. Table 3 shows that a higher density correlates with a lower porosity, as expected.

The filler volume fraction is much lower than the fiber or matrix volume fraction, such that the filler volume fraction is much lower for the composite with fumed alumina incorporation than that with organobentonite incorporation (Table 3). The fiber volume fraction slightly exceeds the matrix volume fraction, which much exceeds the porosity.

As shown in Table 3, the densification of C/C without filler decreases the overall porosity from 16% to 14%. Hence, the densification-accessible porosity in C/C without filler and without densification is 2%. Similarly, the incorporation of fumed alumina to C/C without filler and without densification decreases the total porosity from 16% to 14%, so the fumed-alumina-accessible porosity that in C/C without filler and without densification is 2%. On the other hand, the incorporation of fumed alumina to C/C without filler and without densification decreases the total porosity from 16% to 12%, so that the organobentonite-accessible porosity in C/C without filler and without densification is 4%. The high effectiveness of organobentonite is because the organobentonite functions as both a filler and a binder [1]. The binder action causes the porosity to decrease. In contrast, fumed alumina does not provide any binder function. Nevertheless, the fumed alumina is as effective as a cycle of densification for decreasing the porosity.

Table 3 shows the flexural modulus determined by three-point bending and the longitudinal compressive modulus and displacement per unit load determined by instrumented indentation. A high value of the flexural modulus correlates with a high value of the compressive modulus, though the flexural modulus is higher than the compressive modulus in all cases, as expected. Table 3 also shows that a high flexural strength correlates with a high hardness, a low displacement per unit load, a high flexural modulus and a high compressive modulus. These correlations are as expected and

Table 3
Structure and mechanical properties of C/C composites in the longitudinal direction.

	C/C without filler		C/C with fumed alumina	C/C with organobentonite
Densification	No	Yes	No	No
Thickness (mm)	1.158 ± 0.037	0.933 ± 0.049	0.946 ± 0.069	1.036 ± 0.027
Density (g/cm^3)	1.480 ± 0.038	1.536 ± 0.050	1.540 ± 0.070	1.665 ± 0.022
Matrix porosity (%)[a]	35.7 ± 2.2	31.8 ± 2.1	31.7 ± 2.1	24.2 ± 1.9
Overall porosity (%)[a]	15.8 ± 1.2	14.1 ± 1.1	14.0 ± 1.1	12.0 ± 1.0
Fiber volume fraction (%)[b]	42.8 ± 2.6	44.5 ± 2.8	44.2 ± 2.6	45.4 ± 2.8
Matrix volume fraction (%)[b]	41.7 ± 2.5	41.4 ± 2.7	41.8 ± 2.3	39.2 ± 2.1
Filler volume fraction (%)	0	0	0.5 ± 0.1	3.3 ± 0.5
Flexural strength (MPa)	251.1 ± 10.3	283.8 ± 18.0	326.3 ± 13.8	330.4 ± 15.9
Flexural modulus (GPa)	52.1 ± 4.0	66.4 ± 7.8	69.4 ± 5.5	74.0 ± 7.5
Compressive modulus (GPa)[c]	21.7 ± 2.0	30.4 ± 2.7	38.1 ± 2.5	48.4 ± 0.9
Flexural toughness (MPa)	1.505 ± 0.029	1.285 ± 0.063	0.983 ± 0.051	2.116 ± 0.226
Displacement per unit load (nm/mN)[c]	50.0 ± 3.2	41.3 ± 3.1	38.9 ± 2.8	34.5 ± 2.2
Hardness (GPa)[c]	2.7 ± 0.2	5.0 ± 0.7	5.9 ± 0.3	6.4 ± 0.4

[a] Based on the Rule of Mixtures for the density of the composite, with the carbon matrix in the absence of the porosity assumed to be 1.80 ± 0.05 g/cm^3.
[b] Based on the Rule of Mixtures for the density of the composite, with the density of the carbon fibers being 1.920 ± 0.005 g/cm^3.
[c] Based on instrumented indentation in the longitudinal direction. The maximum load is 10 mN.

support the validity of the flexural testing results.

As shown in Table 3, fumed alumina is the same as the densification in the effectiveness for increasing the flexural modulus (from 52 to 68 GPa), but is more effective than the densification for increasing the longitudinal compressive modulus (to 38 GPa vs. 30 GPa). The fiber-matrix interface is more abused under longitudinal compression than flexure. This suggests that fumed alumina is more effective than the densification for strengthening the fiber-matrix bond.

Table 4 shows that increase of the maximum load used in instrumented indentation decreases the modulus, hardness and fraction of displacement that is reversible. The behavior is similar for the C/C with densification (without filler), C/C with organobentonite and C/C with fumed alumina. The fractional decrease in hardness due to the increase of the maximum load is less significant for the C/C with organobentonite than C/C with fumed alumina or C/C with densification ayr(without filler). This is consistent with the higher modulus of C/C with organobentonite. The behavior is similar between C/C with densification (without filler) and C/C with fumed alumina.

The curves of load vs. displacement during loading and subsequent unloading for various values of the maximum load are shown in Fig. 4 for C/C with fumed alumina and C/C with organobentonite. These curves show that the displacement is mostly reversible upon unloading. In addition, the curves are smooth and do not exhibit any discontinuity. These observations indicate the essential absence of damage up to the highest maximum load of 40 mN.

The thickness of the composite is slightly reduced, the density is slightly increased, the porosity is decreased, the fiber volume fraction is increased slightly, the flexural strength and modulus are increased and the toughness is decreased by densification, as shown for the C/C without filler (Table 3). These effects are as expected. Furthermore, the addition of either organobentonite or fumed alumina as the filler decreases slightly the thickness relative to the C/C without filler and without densification, in addition to increasing the density, decreasing the porosity, increasing the fiber volume fraction slightly, and increasing the flexural strength and modulus (Table 3).

Relative to the C/C without filler but with densification, the organobentonite incorporation essentially does not affect the thickness, density or fiber/matrix volume fraction, but decreases the porosity. The flexural strength, modulus and toughness are all increased. These results are consistent with those of prior work [1].

Relative to the C/C without filler but with densification, the fumed alumina incorporation has negligible effects on the thickness, density, porosity, and the fiber and matrix volume fractions, due to the low filler volume fraction. Nevertheless, the flexural strength is increased substantially, while the flexural modulus is essentially not affected and the toughness is decreased.

The composite with fumed alumina incorporation is similar in strength (330 MPa) but inferior in modulus (70 GPa vs. 74 GPa) and toughness (1.0 MPa vs. 2.1 MPa) and higher in porosity (14% vs. 12%) compared to the composite with organobentonite incorporation. The relatively high porosity of the former is attributed to the nanopores that remain in the fumed alumina after the squishing that occurs during hot pressing. In contrast, the porosity of the composite with organobentonite incorporation is relatively low, probably due to the low porosity in the ceramic-carbon hybrid that

Table 4
Effect of the maximum load on the results of instrumented indentation of composites in the longitudinal direction. The C/C with densification has no filler. The C/C with either filler has undergone no densification.

	Maximum load (mN)	C/C with densification	C/C with fumed alumina	C/C with organobenonite
Modulus (GPa)	10	30.4 ± 2.7	38.1 ± 2.5	48.4 ± 0.9
	20	28.4 ± 1.7	36.3 ± 2.1	46.2 ± 0.4
	30	27.8 ± 1.9	33.5 ± 2.6	45.5 ± 0.5
	40	27.3 ± 2.1	31.1 ± 1.8	44.9 ± 0.7
Hardness (GPa)	10	5.0 ± 0.7	5.9 ± 0.3	6.4 ± 0.4
	20	4.3 ± 0.4	5.1 ± 0.6	6.2 ± 0.3
	30	3.7 ± 0.3	4.2 ± 0.5	5.9 ± 0.7
	40	3.1 ± 0.6	3.6 ± 0.3	5.4 ± 0.3
Fraction of displacement that is reversible (%)	10	70.3 ± 2.3	70.1 ± 1.6	67.8 ± 2.1
	20	69.1 ± 2.1	68.3 ± 1.4	66.5 ± 1.1
	30	67.6 ± 1.3	65.9 ± 1.8	65.3 ± 1.8
	40	65.5 ± 1.2	62.1 ± 1.5	60.7 ± 1.9

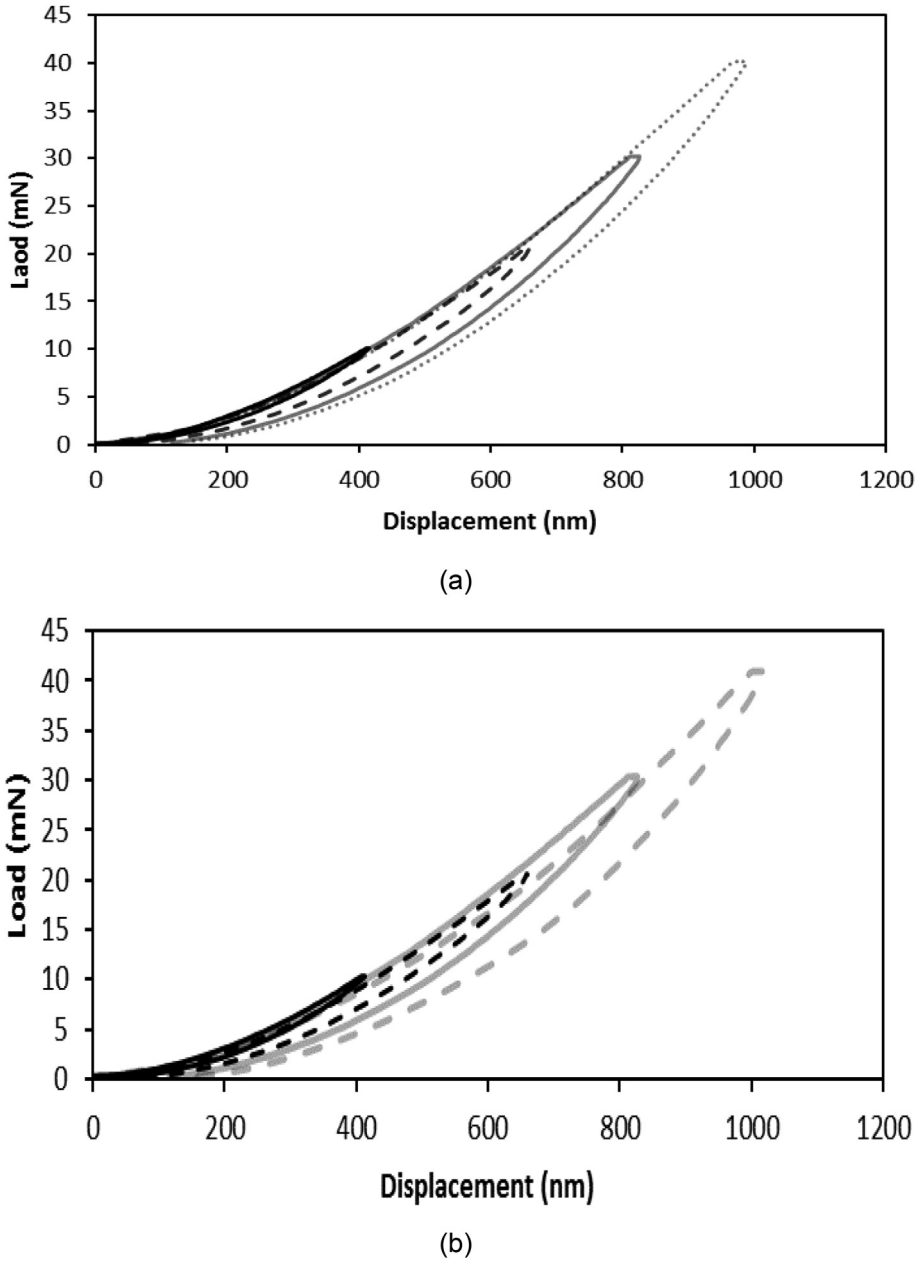

Fig. 4. Curves of load vs. displacement obtained for various values of the maximum load ranging from 10 to 40 mN. Black solid line: up to 10 mN. Black dash line: up to 20 mN. Gray solid line: up to 30 mN. Gray dotted line: up to 40 mN. (a) C/C with fumed alumina. (b) C/C with organobentonite.

results from hot-pressing organobentonite [1]. The modulus is slightly higher (though within the data scatter) for the composite with organobentonite than that with fumed alumina, in spite of the high modulus of alumina (375 GPa [20]) compared to that of clay (5–16 GPa [21]) or hot-pressed organobentonite (69 GPa [1]). This is attributed to the relatively strong filler-matrix bonding for the composite with organobentonite, due to the fact that organobentonite serves as both filler and binder. The strength is similar for the composite with organobentonite and that with fumed alumina, in spite of the relatively high porosity of the latter.

Organobentonite increases the toughness to 2.1 MPa, whereas fumed alumina decreases the toughness to 1.0 MPa. The high toughening ability of organobentonite is attributed to the nanostructure of the ceramic-carbon hybrid that results from hot-pressing the organobentontite and the high volume fraction of organobentonite compared to that of fumed alumina. The negative effect of fumed alumina on the toughness probably relates to the aggregate structure of fumed alumina and the limited movement of the primary particles in an aggregate relative to one another. Due to the ionic bonding in alumina, the movement of the primary particles in an aggregate of fumed alumina is more difficult than that of the primary particles in an aggregate of carbon black [12]. In spite of its low volume fraction, fumed alumina gives similar effects on the C/C flexural strength and modulus as organobentonite.

Due to its low volume fraction (0.5%) and compacted nanostructure (with the compacted fumed alumina conforming to the topography of the laminae), the fumed alumina cannot be discerned in the C/C. In contrast, the organobentonite can be discerned in case of C/C with organibentonite [1]. The microstructure is similar for C/C with fumed alumina and C/C without filler but with

densification. As shown in Table 3, both the fiber volume fraction and the porosity are essentially the same for the two types of composite.

In spite of the subtle nature of the presence of the fumed alumina in the C/C, the fumed alumina enhances significantly the flexural strength of the C/C, though its enhancement of the modulus is less significant, as shown in Table 3. This mechanical effect of the fumed alumina incorporation suggests that the pore structure in the C/C with fumed alumina is more refined than that in C/C without filler but with densification. The refined pore structure of the C/C with fumed alumina is expected, due to (i) the conformability and spreadability of fumed alumina causing the porosity in the matrix (including that at the fiber-matrix interface) to be reduced in terms of both the total pore volume and the mean pore size, and (ii) the relatively minor level of porosity introduced by the presence of fumed alumina is in the nanoscale. It is well-known that, for a brittle material, the pores are detrimental to the strength and are less detrimental to the modulus, and the refinement of the pore structure helps make the pores less detrimental, thereby enhancing the strength.

The refined pore structure is also attractive for lowering the density of the composite. Thus, in spite of its relatively low density of 1.54 g/cm^3, the C/C with fumed alumina exhibits relatively high flexural strength. In contrast, the C/C with organobentonite exhibits a relatively high density of 1.67 g/cm^3 and a relatively low porosity, but its flexural strength is essentially the same as that of the C/C with fumed alumina.

The density has commonly been used in the field of C/C as an indicator of the quality of the composite, due to the fact that the mechanical properties of C/C improve with increasing degree of densification. However, this work shows that a relatively high quality C/C can be obtained at a relatively low density, provided that the pore structure is sufficiently refined, as in the case of the C/C with fumed alumina.

Table 5 shows the flexural strength and modulus of each constituent (fiber, matrix and filler), as calculated based on the Rule of Mixtures for the strength/modulus. This Rule is based on the assumed notion that the fibers and matrix are parallel to the stress (in-plane), such that this parallel combination is either parallel or perpendicular to the direction of continuity of the filler. The fiber flexural strength of 530 MPa is low compared to the known fiber tensile strength of 1560 MPa. The fiber flexural modulus of 102 GPa is lower than the known fiber tensile modulus of 159 GPa. This large difference is attributed to the inadequate fiber alignment. It is also due to the fact that the compressive strength is much lower than the tensile strength of carbon fibers, so that the flexural strength is lower than the tensile strength. The flexural strength and modulus of the matrix are lower than those of the fibers, as expected, due to the relatively low carbonization temperature of 1000 °C.

The calculated strength/modulus of either filler is high compared to values expected for such ceramic materials, in the case that the filler is considered to be continuous and parallel to the fibers, whereas it is negative in the case that the filler is considered to be continuous and perpendicular to the fibers. The negative values are not meaningful. Nevertheless, the results indicate that the actual filler properties are lower than the values calculated by assuming that the filler is continuous and parallel to the fibers, as expected. Furthermore, the results indicate that the parallel model is closer to reality than the perpendicular model.

Table 6 shows the filler modulus calculated from the measured composite modulus based on the Hashin–Shtrikman model, which is found to be superior to the Rule of Mixtures (Table 5). The two constituents in the C/C are considered as the filler and the C/C without filler (but with densification, 66.4 ± 7.8 GPa). The measured modulus of the C/C with the filler is then used to back out the modulus of the filler. The calculation according to the Hashin–Shtrikman model requires the Poisson's ratio of the filler. For the hot-pressed organobentonite, the Poisson's ratio is assumed to be the same as that of mullite, which is 0.28 [22]; for fumed alumina, the Poisson's ratio is assumed to be the same as that of alumina, which is 0.24 [23]; for the C/C without filler, the Poisson's ratio is assumed to be the same as that of graphite, which is 0.18 [17].

Based on the Hashin–Shtrikman upper and lower bounds, the modulus of fumed alumina itself is estimated to range from 41 to 69 GPa. These are below the value of 375 GPa for conventional dense alumina [20]. The difference in modulus is probably due to the difference in crystallinity and microstructure between the alumina in fumed alumina and conventional dense alumina. In spite of its presumably non-ideal structure, fumed alumina is effective for enhancing the C/C flexural modulus and strength relative to the corresponding composite without this filler (also without densification). In fact, the flexural strength provided by the fumed alumina addition is even higher than that of the C/C without filler but with densification.

Based on the Hashin–Shtrikman upper and lower bounds, the modulus of hot-pressed organobentonite is estimated to range from 27 to 80 GPa. These values are above those ranging from 5 to 16 GPa for clay [21] and are consistent with the previously reported value of 69 GPa for this filler [1].

This paper uses unidirectional composites to demonstrate the positive effects of fumed alumina incorporation. However, fumed alumina incorporation using the basic method described in this paper is expected to be applicable to composites with various fiber lay-up configurations.

4. Conclusions

This paper provides the first report of the incorporation of fumed alumina in C/C. The fumed alumina is in the form of aggregated nanoparticles with aggregate size 100–200 nm and average pore size 15 nm. Due to this structure, fumed alumina is squishable, and hence conformable and spreadable. The conformability and spreadability are attractive for reducing the porosity in the composite. In contrast, organobentonite is not squishable, though it is unusual in its ability to function as both a filler and a binder [1]. The fumed-alumina-accessible porosity is 2% (equal to

Table 5
Flexural strength/modulus of each constituent of a C/C composite, as calculated based on the measured composite strength/modulus and the Rule of Mixtures for the strength/modulus. This Rule is based on the assumed notion that the fibers and matrix are parallel to the stress (in-plane), such that this parallel combination is either parallel or perpendicular to the direction of continuity of the filler. The filler is actually not continuous.

Flexural property[a]	Fibers	Matrix	Organobentonite		Fumed alumina	
			Parallel	Perpendicular	Parallel	Perpendicular
Strength (MPa)	530 ± 59	57.8 ± 2.8	2007 ± 146	−40.1 ± 2.8	13611 ± 466	−5.6 ± 1.0
Modulus (GPa)	103 ± 18	31.4 ± 2.1	752 ± 80	−4.9 ± 0.8	2164 ± 39	−1.1 ± 0.3

[a] Calculated using the constituent volume fractions shown in Table 3.

Table 6
Flexural modulus of the filler in C/C, as estimated from the Hashin–Shtrikman upper and lower bounds.

		C/C with fumed alumina	C/C with organobentonite
Composite flexural modulus (GPa)		69.4 ± 5.5	74.0 ± 7.5
Composite porosity (%)		14.0 ± 1.1	12.0 ± 1.0
Filler modulus (GPa)	Upper bound	79.8 ± 8.1	68.9 ± 6.2
	Lower bound	26.9 ± 7.5	40.5 ± 5.4

the one-cycle-densification-accessible porosity), while the organobentonite-accessible porosity is 4%, in C/C without filler and without densification.

The incorporation of fumed alumina (0.5 vol.% or 1.1 wt.%) in unidirectional C/C (44 vol.% fibers, 42 vol.% matrix and 14 vol.% porosity) fabricated from pitch-based carbon fiber and mesophase pitch carbon matrix precursor by hot-press carbonization at 1000 °C and 21 MPa improves the oxidation resistance (tested by thermogravimetry up to 1000 °C), flexural strength, flexural modulus, longitudinal compressive modulus and longitudinal hardness of the composite, in addition to decreasing the longitudinal displacement per unit load. Even without densification, the oxidation resistance, flexural strength (330 MPa) and longitudinal compressive modulus (38 GPa) achieved with fumed alumina incorporation are superior, the longitudinal displacement per unit load is smaller, and the flexural modulus, longitudinal hardness and porosity are similar to those of the corresponding composite without filler but with densification (flexural strength 280 MPa and longitudinal compressive modulus 30 GPa). However, the flexural toughness (1.0 MPa) is lower than the composite without filler but with densification (1.3 MPa).

Relative to the C/C without filler but with densification, the positive effect of fumed alumina on the oxidation resistance and the flexural strength is attributed to the pore structure refinement and the consequent reduced accessibility of air to the C/C. The total porosity is the same for the C/C with fumed alumina but without densification and for the C/C without filler but with densification.

Fumed alumina (0.5 vol.% or 1.1 wt.%) is more effective than organobentonite (3.3. vol.% or 6.4 wt.%) for improving the oxidation resistance, in spite of the higher porosity of the composite with fumed alumina (14% versus 12%). The oxidation resistance achieved by organobentonite incorporation without densification is inferior to that of the corresponding composite without filler but with densification. This work shows that a relatively high quality C/C can be obtained at a relatively high porosity, provided that the pore structure is sufficiently refined, as in the case of the C/C with fumed alumina.

Fumed alumina is inferior to organobentonite for increasing the flexural modulus (70 GPa vs. 74 GPa) or the longitudinal compressive modulus (38 GPa vs. 48 GPa), though the flexural strength, longitudinal hardness and longitudinal displacement per unit load provided by the two fillers are similar (strength 330 MPa, hardness 6 GPa, and displacement per unit load 37 nm/mN). Organobentonite increases the toughness to 2.1 MPa, whereas fumed alumina decreases the toughness to 1.0 MPa, relative to the composite without filler (whether with or without densification).

Based on the Hashin–Shtrikman upper and lower bounds, the modulus of fumed alumina itself is estimated to range from 41 to 69 GPa. This value is low compared to the value for conventional solid alumina. On the other hand, the bounds similarly obtained for hot-pressed organobentonite as a filler are consistent with the previously reported measured value of this material in monolithic form [1].

Acknowledgment

The authors are thankful to Dr. Yoshihiro Takizawa and Mr. Ailipati Delixiati of University at Buffalo, State University of New York, for technical assistance.

References

[1] A. Wang, X. Gao, R.F. Giese, D.D.L. Chung, A ceramic-carbon hybrid as a high-temperature structural monolith and reinforcing filler and binder for carbon/carbon composites, Carbon 59 (2013) 76–92.
[2] J.H. Koo, S.C. Lao, H.K. Jor, L.A. Pilato, G.E. Wissler, J. Lee, Z. Luo, Thermo-oxidative studies of nanomodified carbon/carbon composites, in: Proc. American Society for Composites, Technical Conference, Vol. 22nd, 2007, pp. 117/1–117/20.
[3] Y. Cai, S. Fan, H. Liu, L. Zhang, L. Cheng, J. Jiang, B. Dong, Mechanical properties of a 3D needled C/SiC composite with graphite filler, Mater Sci. Eng. A 527 (2010) 539–543.
[4] T. Ko, W. Kuo, W. Han, T. Day, Modification of a carbon/carbon composite with a thermosetting resin precursor as a matrix by the addition of carbon black, J. Appl. Polym. Sci. 102 (2006) 333–337.
[5] J. Lin, C.M. Ma, N. Tai, W. Wu, C. Chen, Preparation and properties of SiC modified carbon/carbon composites by carbothermal reduction reaction, J. Mater Sci. Lett. 18 (1999) 1353–1355.
[6] W. Kowbel, C. Bruce, J.C. Withers, P.O. Ransome, Effect of carbon fabric whiskerization on mechanical properties of C-C composites, Compos. Part A 28A (1997) 993–1000.
[7] R. Jain, U.K. Vaidya, A. Haque, Processing and characterization of carbon-carbon nanofiber composites, Adv. Compos. Mater 15 (2) (2006) 211–241.
[8] P. Xiao, X. Lu, Y. Liu, L. He, Effect of in situ grown carbon nanotubes on the structure and mechanical properties of unidirectional carbon/carbon composites, Mater Sci. Eng. A 528 (2011) 3056–3061.
[9] P. Somasundaran, Encyclopedia of Surface and Colloid Science, second ed., vol. 7, CRC Press, Boca Raton, FL, 2006, p. 5317.
[10] I.C. Halalay, M.J. Lukitsch, M.P. Balogh, C.A. Wong, Nanoindentation testing of separators for lithium-ion batteries, J. Power Sources 238 (2013) 469–477.
[11] C. Lin, D.D.L. Chung, Nanostructured fumed metal oxides for thermal interface pastes, J. Mater Sci. 42 (22) (2007) 9245–9255.
[12] C. Lin, D.D.L. Chung, Rheological behavior of thermal interface pastes, J. Electron Mater 38 (10) (2009) 2069–2084.
[13] C. Lin, D.D.L. Chung, Nanoclay paste as thermal interface material for smooth surfaces, J. Electron Mater 37 (11) (2008) 1698–1709.
[14] http://www.msm.cam.ac.uk/mechtest/docs/XP%20User's%20Manual.pdf, as viewed on Dec. 16, 2014.
[15] A.C. Fischer-Cripps, Critical review of analysis and interpretation of nano-indentation test data, Surf. Coat. Technol. 200 (2006) 4153–4165.
[16] A. Eloranta, Experimental Methods for Measuring Elasto-plastic Parameters of Bentonite Clay, Master's Thesis, University of Jyvaskla, 2012, pp. 38–42.
[17] B.T. Kelly, Physics of Graphite, Applied Science Publishers, London, 1981, pp. 43–44.
[18] L. Qiana, M. Lib, Z. Zhoua, H. Yanga, X. Shi, Comparison of nano-indentation hardness to microhardness, Surf. Coatings Technol 195 (2005) 264–271.
[19] Y. Takizawa, D.D.L. Chung, Fumed-alumina-derived nanoporous alumina as a new low-k dielectric material for microelectronic packaging, J. Electron. Mater 44 (7) (2015) 2211–2220.
[20] Accuratus. http://accuratus.com/alumox.html. (accessed 03.01.15).
[21] Bathija AP, Elastic Properties of Clay, http://inside.mines.edu/UserFiles/File/CRA/Thesis/Arpita_Pal_Bathija_Thesis.pdf. (accessed 03.01.15).
[22] S. Crudele, W. Kriven, Elastic properties of mullite, J. Am. Ceram. Soc. 81 (4) (1998) 1025–1028.
[23] P. Auerkari, Mechanical and Physical Properties of Engineering Alumina Ceramics, VTT Manufacturing Technology, Technical Research Centre of Finland, 1996, pp. 14–15.